

Shear and vorticity in the spherical collapse of dark matter haloes

Robert Reischke¹★, Francesco Pace², Sven Meyer³ and Björn Malte Schäfer¹

¹ *Zentrum für Astronomie der Universität Heidelberg, Astronomisches Recheninstitut, Philosophenweg 12, 69120 Heidelberg, Germany*

² *Jodrell Bank Centre for Astrophysics, School of Physics and Astronomy, The University of Manchester, Manchester, M13 9PL, United Kingdom*

³ *Zentrum für Astronomie der Universität Heidelberg, Institut für theoretische Astrophysik, Philosophenweg 12, D-69120, Heidelberg, Germany*

2016

ABSTRACT

We study the evolution of spherical symmetric overdense regions in tidal gravitational fields. The evolution of the overdensity is governed by the Raychaudhuri equation, sourced by self gravity and external fields, the latter are described by first order Lagrangian perturbation theory. The tidal tensor is decomposed into a symmetric and anti-symmetric part, using the commutator and the anti-commutator with the inertia tensor respectively which are then identified with shear and rotation.

The inertia tensor is obtained from the curvature of the density field, which is correlated with the values of the tidal tensor. By estimating by how much an ellipsoidal region of the same mass as the spherical region would spin up due to the misalignment of the eigenframes of the inertia and tidal tensor, i.e. tidal torquing, we are able to identify the invariants σ^2 and ω^2 induced by the external gravitational tidal field.

Within this framework we find that $\omega^2 \leq \sigma^2$ holds exactly and not only in a statistical sense if we restrict our considerations to maxima in the density field. This shows that the collapse will always proceed faster than in the case without tidal gravitational field. We also investigate their scaling with mass and the influence on δ_c and find similar results as in Reischke et al. (2016a), namely roughly one percent deviations from the standard spherical collapse model. As a consequence, cluster counts could build up an additional $\sim 1\sigma$ in cosmological parameters.

Key words: Cosmology: theory; Methods: analytical

1 INTRODUCTION

The combined observations of type-Ia supernovae (e.g. Riess et al. 1998; Perlmutter et al. 1999), the cosmic microwave background (e.g. Komatsu et al. 2011; Planck Collaboration et al. 2016), the Hubble constant and large-scale structure (e.g. Cole et al. 2005) show that the universe is spatially flat and expanding in an accelerated fashion. Under the assumptions of General Relativity being true and the symmetries of the Friedmann-Robertson-Walker metric, the accelerated expansion can be described by the cosmological constant Λ or by adding a fluid component (see e.g. Copeland et al. 2006, for a review) to the energy-momentum content of the Universe with an equation of state $w < -1/3$ which may be time dependent. In this scenario, generally called dark energy, Λ would corresponds to a constant $w = -1$.

The equation of state parameter, as well as the other parameters such as the dark energy content Ω_Λ or the matter content Ω_m of the cosmological standard model can and already have been measured to very high precision. However, with high precision comes also the risk of possible biases in the parameters if the theoretical prediction and astrophysics are not modelled well enough. It

is therefore necessary to review and perhaps modify common concepts and models since possible systematics are no longer wiped out by the statistical errors of the experiment.

The halo mass function is, due to its exponential sensitivity, one of the main tools to provide robust theoretical predictions for many observables such as cluster counts (Sunyaev & Zeldovich 1980; Majumdar 2004; Diego & Majumdar 2004; Fang & Haiman 2007; Abramo et al. 2009; Angrick & Bartelmann 2009) or weak lensing peak counts (Maturi et al. 2010; Maturi et al. 2011; Lin & Kilbinger 2014; Reischke et al. 2016b). As it deals with objects in the highly non-linear regime one needs to extrapolate the linearly evolved density to the non-linear one which is encoded in the critical linear overdensity δ_c . This can be done by using the spherical collapse model introduced by Gunn & Gott (1972) and later extended in several works (Fillmore & Goldreich 1984; Bertschinger 1985; Ryden & Gunn 1987; Avila-Reese et al. 1998; Mota & van de Bruck 2004; Abramo et al. 2007; Pace et al. 2010, 2014a). This model assumes in its most simplistic form, called standard spherical collapse (SPC hereafter), the evolution of a spherically symmetric density perturbation in an expanding background with uniform background density, i.e. an isolated collapse. The overdensity grows until it reaches a critical point at which it starts to collapse under its own gravity. Due to the collapse it decouples from the ex-

★ e-mail: reischke@stud.uni-heidelberg.de

pansion. In theory the overdense region would collapse to a single point, however, the energy released during the collapse is converted into random motions of the particles, such that an equilibrium situation (in the sense of virialized structure, Schäfer & Koyama 2008) is created.

It is necessary to check the validity of the SPC model and introduce additional effects subject to more realistic situations. One of the ingredients of the SPC model is the embedding of the spherical region into a uniform background. In this way no external forces can act on the halo by virtue of Birkhoff's theorem. However, halos are embedded in a random field giving rise to gravitational tidal fields. The shear effects induced by those external tidal fields have been investigated in Reischke et al. (2016a, R16 from now on) for dark energy models and clustering dark energy models in Pace et al. (2016) leading to a distribution in δ_c instead of a single, distinct value determined by the background cosmology. By using Lagrangian perturbation theory (Zel'Dovich 1970) for the surrounding tidal fields the approach used there is not based on phenomenological models and yields a description from first principles in its range of validity. In Del Popolo et al. (2013a,b); Pace et al. (2014b) a phenomenological model was used, jointly describing the effect of shear and rotation by introducing an additional term to match the Newtonian predictions.

In this paper we extend the work done in R16 by not only describing the induced shear but also induced rotation by external tidal fields. The latter will be done by relaxing the assumption of spherical symmetry prior to collapse leading to a possible spin up of the halo prior to collapse by tidal torquing as described in Schäfer (2009); Schäfer & Merkel (2012). This will naturally lead to an effective reduction of the effect described in R16. However by introducing more random variables by the inclusion of the inertia tensor which itself is given by the curvature of the density field additional correlations will influence the random process outlined in R16.

The structure of the paper is as follows. In section 2 we very briefly review the spherical collapse model and show the equations to be solved. In section 3 we introduce the statistical procedure to obtain tidal shear values and decompose them to identify the shear and rotation tensor respectively. The obtained invariants are then used in section 4 to calculate the influence of the tidal fields on δ_c for the standard Λ CDM model. During the whole paper we compare our results with R16. We summarize our findings in section 5.

2 SPHERICAL COLLAPSE

The spherical collapse model has been discussed by various authors, e.g. Bernardeau (1994); Padmanabhan (1996); Ohta et al. (2003, 2004); Abramo et al. (2007) and Pace et al. (2010, 2014a). The perturbed hydrodynamical equations read:

$$\begin{aligned} \dot{\delta} + (1 + \delta)\nabla_x \mathbf{u} &= 0, \\ \ddot{\mathbf{u}} + 2H\mathbf{u} + (\mathbf{u} \cdot \nabla_x)\mathbf{u} &= -\frac{1}{a^2}\nabla_x\phi, \\ \nabla_x^2\phi &= 4\pi G a^2 \rho_0 \delta, \end{aligned} \quad (1)$$

with comoving coordinate \mathbf{x} , comoving peculiar velocity \mathbf{u} , Newtonian potential ϕ , overdensity δ and background density ρ_0 , respectively. Here the dot represents a derivative with respect to cosmic time t . Taking the divergence of the Euler equation and inserting

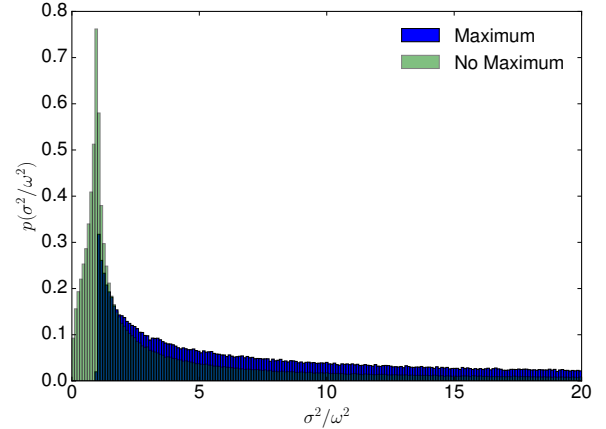


Figure 1. Distributions of the ratio of the two invariants σ^2 and ω^2 . The green histogram does not include the maximum constraint, i.e. $\lambda_i > 0$, while the blue histogram includes this constraint. Clearly the constraint moves all values which would have $\sigma^2 < \omega^2$ to values $\sigma^2 > \omega^2$ as it is expected from the analytical considerations made in Eq. (32). The smoothing length for the power spectrum is $R = 10 \text{ Mpc} h^{-1}$.

the Poisson equation yields

$$\begin{aligned} \dot{\delta} &= -(1 + \delta)\theta, \\ \dot{\theta} &= -2H\theta - 4\pi G \rho_0 \delta - \frac{1}{3}\theta^2 - (\sigma^2 - \omega^2). \end{aligned} \quad (2)$$

Here we used the decomposition

$$\nabla_x \cdot [(\mathbf{u} \nabla_x)\mathbf{u}] = \frac{1}{3}\theta^2 + \sigma^2 - \omega^2, \quad (3)$$

with the expansion $\theta = \nabla_x \cdot \mathbf{u}$, the shear $\sigma^2 \equiv \sigma_{ij}\sigma^{ij}$ and the rotation $\omega^2 \equiv \omega_{ij}\omega^{ij}$ under the assumption of a top-hat profile. The rotation and the shear tensors are themselves the antisymmetric and the symmetric traceless part of the velocity divergence tensor, respectively. They are defined as

$$\begin{aligned} \sigma_{ij} &= \frac{1}{2}(\partial_i u_j + \partial_j u_i) - \frac{\theta}{3}\delta_{ij}, \\ \omega_{ij} &= \frac{1}{2}(\partial_i u_j - \partial_j u_i), \end{aligned} \quad (4)$$

where $\partial_i \equiv \partial/\partial x^i$. We now use the relation $\partial_t = aH(a)\partial_a$ and $f = 1/\delta$ which leads to

$$\begin{aligned} f' &= \frac{\theta}{aH}f(1 + f), \\ \theta' &= -\frac{2\theta}{a} - \frac{3H\Omega_m}{2af} - \left(\frac{1}{3}\theta^2 + \sigma^2 - \omega^2\right)\frac{1}{aH}. \end{aligned} \quad (5)$$

The system defined in Eq. (5) is solved numerically until $f \sim 10^{-8}$ and then it is extrapolated to zero, which is much more stable than treating the system in δ instead of f . This yields the appropriate initial conditions for the linear version of 5 which gives δ_c . Usually σ^2 and ω^2 are neglected, however, their influence has phenomenologically been investigated, e.g. by Del Popolo et al. (2013a,b) in the Λ CDM and dark energy cosmologies and by Pace et al. (2014b) in clustering dark energy models.

3 ROTATION AND SHEAR

In this section we describe how external tidal fields introduce interactions, leading to shearing and rotational effects. For this we

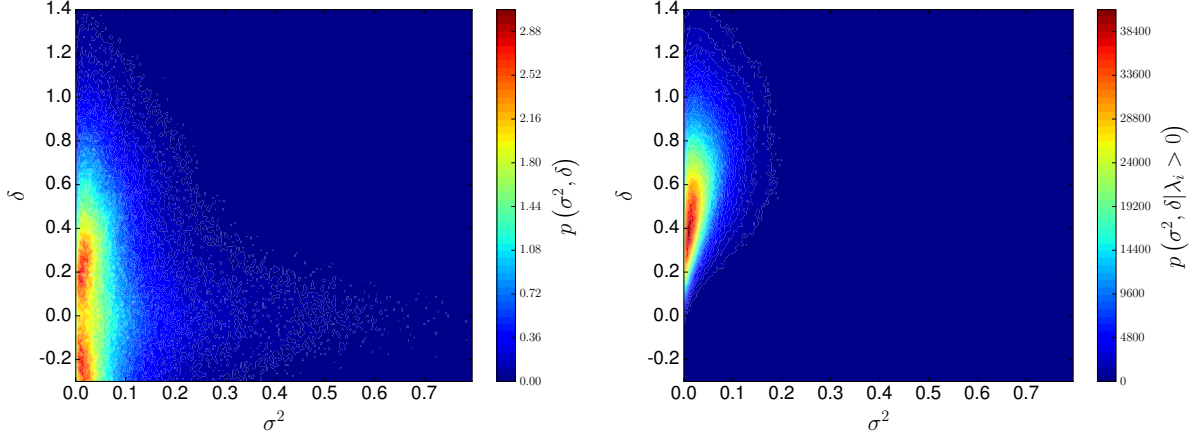


Figure 2. Joint distributions (not normalized) of the density contrast $\delta = \text{tr}(\Psi)$ and the invariant σ^2 . *Left panel:* No maximum constraint. The distribution is similar to the distribution found in R16. *Right panel:* The maximum constraint is imposed. Clearly the constraint enforces higher values of δ and thus also in σ^2 , which is due to the correlations in the y_{lm}^n basis given in Eq. (11). The smoothing length for the power spectrum is $R = 10 \text{ Mpc} h^{-1}$.

expand the formalism from R16 to generate values for the gravitational tidal field represented by the tidal tensor Ψ from the statistics of the density field, i.e. its power spectrum, using the Zel’dovich approximation (Zel’dovich 1970). We therefore assume that the shear values can be sampled from a Gaussian random field. This tidal field will then give rise to shear effects which act on the protohalo via the invariant σ^2 . As long as the protohalo is assumed to be spherical the eigensystem of its inertia tensor I can always be chosen to coincide with the eigensystem of Ψ . We now assume the protohalo to be ellipsoidal prior to collapse and sample the eigenvalues of its inertia tensor from the curvature of the density field. In this way I and Ψ will no longer commute and the protohalo can gain angular momentum via the mechanism of tidal torquing. This procedure essentially means that we place an elliptical test particle (with internal dynamics still governed by the spherical collapse equations) into a non-uniform density field which can act on the internal dynamics via its invariants.

We will quickly review the random process for Ψ and the theory of tidal torquing and show how the two invariants σ^2 and ω^2 can be identified.

3.1 Generating shear values

For scales large enough, particles follow Zel’dovich trajectories (Zel’dovich 1970)

$$x_i = q_i - D_+(t) \partial_i \psi \equiv q_i - D_+(t) \psi_{,i} . \quad (6)$$

The displacement field ψ is related to the density contrast δ via a Poisson relation, $\Delta \psi = \delta$. In Fourier space we can thus write

$$\psi_{,ij} = - \int \frac{d^3 k}{(2\pi)^3} \frac{k_i k_j}{k^2} \delta(\mathbf{k}) \exp(i\mathbf{k}\mathbf{x}) . \quad (7)$$

In spherical coordinates (Regős & Szalay 1995; Heavens & Sheth 1999) we can consider the peaks symmetric about the origin on the z -axis and introduce dimensionless complex variables

$$y_{lm}^n = \sqrt{4\pi} \frac{i^{l+2n}}{\sigma_{l+2n}} \int \frac{d^3 k}{(2\pi)^3} k^{l+2n} \delta(\mathbf{k}) Y_{lm}(\hat{k}) \exp(i\mathbf{k}\mathbf{x}) , \quad (8)$$

with the direction vector $\hat{k} = \mathbf{k}/k$ and σ_i being the spectral moments of the matter power spectrum

$$\sigma_i^2 = \frac{1}{2\pi^2} \int dk k^{2i+2} P(k) . \quad (9)$$

and Y_{lm} are the spherical harmonics. With this we obtain a linear relation (Schäfer & Merkel 2012) between y_{lm}^n and the tidal values $\psi_{,ij}$

$$\begin{aligned} \sigma_0 y_{20}^{-1} &= - \sqrt{\frac{5}{4}} (\psi_{,xx} + \psi_{,yy} - 2\psi_{,zz}) , \\ \sigma_0 y_{2\pm 1}^{-1} &= - \sqrt{\frac{15}{2}} (\psi_{,xz} \pm i\psi_{,yz}) , \\ \sigma_0 y_{2\pm 2}^{-1} &= \sqrt{\frac{15}{8}} (\psi_{,xx} - \psi_{,yy} \pm 2i\psi_{,xy}) , \\ \sigma_0 y_{00}^0 &= (\psi_{,xx} + \psi_{,yy} + \psi_{,zz}) . \end{aligned} \quad (10)$$

The variables y_{lm}^n now have a diagonal auto-correlation matrix:

$$\langle y_{lm}^n(\mathbf{x}) y_{l'm'}^{n'}(\mathbf{x})^* \rangle = (-1)^{n-n'} \frac{\sigma_{l+n+n'}^2}{\sigma_{l+2n} \sigma_{l+2n'}} \delta_{ll'} \delta_{mm'} . \quad (11)$$

By inverting the linear relation, we can draw random samples in the y_{lm}^n basis and calculate the components of the tidal tensor $\Psi_{ij} \equiv \psi_{,ij}$. The strength of the tidal field depends on the characteristic length scale $R(M)$ of the halo and thus on its mass. We thus introduce a low-pass filter to cut off high frequency modes, suppressing fluctuations on scales smaller than the characteristic scale of the halo:

$$P(k) \rightarrow P(k) W_R^2(k) , \quad (12)$$

with $W_R(k) = \exp(-k^2 R^2/2)$. The mass scale is obtained via $M = \frac{4\pi}{3} \rho_{\text{crit}} \Omega_m R^3$, where $\rho_{\text{crit}} = 3H^2/(8\pi G)$ is the critical density. For more details on the tidal field and the random process we refer to R16.

3.2 Tidal Torquing

In the picture of tidal torquing angular momentum is generated by the tidal gravitational field which exerts a torquing moment on the protohalo. It is important to note that the vorticity ω is not driven by

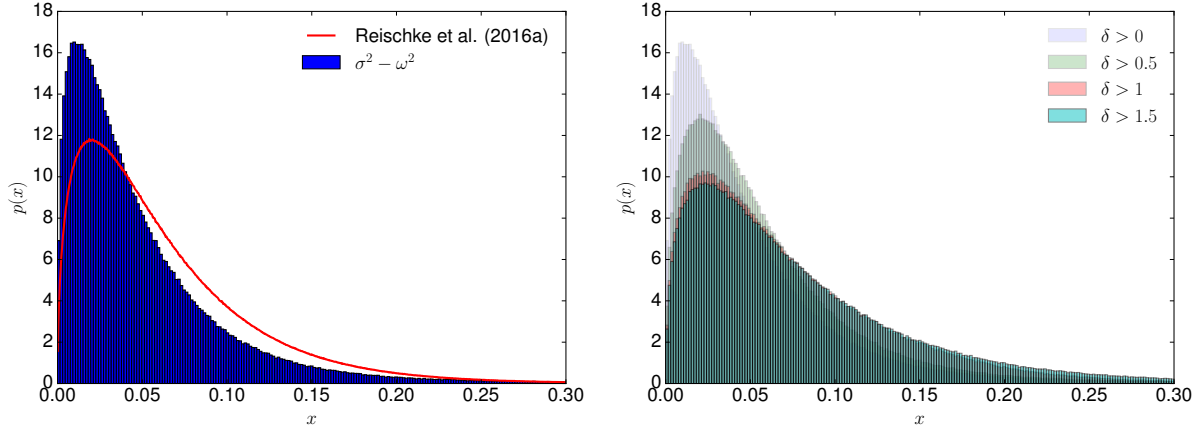


Figure 3. *Left panel:* Distributions of the invariants $x \equiv \sigma^2 - \omega^2$ (blue histogram) and R16 (red curve) on a scale $R = 10 \text{ Mpc h}^{-1}$ and a threshold $\delta > 0$. Although this work has larger shear values in general due to the maximum constraint, they get partially erased due to the rotation of the protohalo. This results into a smaller contribution to the collapse than in R16. *Right panel:* Distributions of the invariants $\sigma^2 - \omega^2$ for different thresholds δ on a scale of $R = 10 \text{ Mpc h}^{-1}$. Higher peaks induce higher values for $\sigma^2 - \omega^2$.

the non-linear term $\nabla \times (\mathbf{v} \times \boldsymbol{\omega})$ in the Euler equation. On the contrary, the angular momentum is generated by vorticity-free flows generating shear effects on the protohalo prior to collapse. During this process the halo is slightly deformed and tends to align its inertia tensor in the eigenframe of the shear tensor. After decoupling from the shear flow and the start of collapse the length of the lever arms reduces dramatically making tidal torquing inefficient. Therefore, the angular momentum just before collapse begins is a good proxy for the total rotation of the halo.

The angular momentum \mathbf{L} of a rotating mass distribution $\rho(\mathbf{r}, t)$ is given by

$$\mathbf{L}(t) = \int_V d^3r (\mathbf{r} - \bar{\mathbf{r}}) \times \mathbf{v}(\mathbf{r}, t) \rho(\mathbf{r}, t), \quad (13)$$

with \mathbf{v} being the rotational velocity and V the physical volume under consideration. Making use of the Zel'dovich approximation and expressing everything in the Lagrangian-frame (i.e. comoving), the angular momentum becomes

$$\mathbf{L} = \rho_0 a^5 \int_{V_L} d^3q (\mathbf{q} - \bar{\mathbf{q}}) \times \dot{\mathbf{x}}, \quad (14)$$

neglecting higher order terms (White 1984; Catelan & Theuns 1996; Crittenden et al. 2001). The velocity $\dot{\mathbf{x}}$ is given via the gradient of the potential ψ , which can be expanded in the vicinity of the centre of gravity $\bar{\mathbf{q}}$ if its variation across V_L is small:

$$\partial_i \psi(\mathbf{q}) \approx \partial_i \psi(\mathbf{q})|_{\mathbf{q}=\bar{\mathbf{q}}} + \partial_{ij} \psi(\mathbf{q})|_{\mathbf{q}=\bar{\mathbf{q}}} (\mathbf{q} - \bar{\mathbf{q}})_j, \quad (15)$$

with expansion coefficients $\psi_{ij} \equiv \partial_{ij} \psi$ describing the tidal shear given in Eq. (10). The first term can be neglected as it only describes the displacement of the protohalo, the second however will be responsible for rotational effects. Introducing the inertial tensor I_{ij} as

$$I_{ij} = \rho_0 a^3 \int_{V_L} d^3q (\mathbf{q} - \bar{\mathbf{q}})_i (\mathbf{q} - \bar{\mathbf{q}})_j, \quad (16)$$

the angular momentum can be written as

$$L_i = a^2 \dot{D}_+ \epsilon_{ijk} I_{jl} \psi_{lk}, \quad (17)$$

with the Levi-Civita symbol ϵ_{ijk} . The matrix product in the latter expression $\mathbf{X} = \mathbf{I} \boldsymbol{\Psi}$ can be decomposed in a symmetric \mathbf{X}^+ and

anti-symmetric part \mathbf{X}^- defined via the anti-commutator and the commutator respectively:

$$\mathbf{X}^+ \equiv \frac{1}{2} \{\mathbf{I}, \boldsymbol{\Psi}\}, \quad \mathbf{X}^- \equiv \frac{1}{2} [\mathbf{I}, \boldsymbol{\Psi}]. \quad (18)$$

With this definition the angular momentum can be written as (Schäfer 2009; Schäfer & Merkel 2012)

$$L_i = a^2 \dot{D}_+ \epsilon_{ijk} X_{jk} = a^2 \dot{D}_+ \epsilon_{ijk} X_{jk}^-, \quad (19)$$

since the contraction with ϵ_{ijk} will only pick out the anti-symmetric part of \mathbf{X} . Thus, angular momentum is not generated if inertia and tidal shear have a common eigensystem, which is always the case for a matter distribution invariant under $\text{SO}(3)$, therefore we need to have $\mathbf{X}^- \neq 0$ to generate angular momentum. On the other hand \mathbf{X}^+ will measure the alignment of the eigensystems of inertia and shear and thus cause shear effects due to deformations.

The components of the inertial tensor \mathbf{I} can be expressed via second derivatives of the density field $\delta(\mathbf{x})$ which are given by

$$\delta_{ij} = \int \frac{d^3k}{(2\pi)^3} k_i k_j \delta(\mathbf{k}) \exp(i\mathbf{k}\mathbf{x}). \quad (20)$$

Thus the decomposition works in the same way as before:

$$\begin{aligned} \sigma_{2y_{20}}^0 &= -\sqrt{5/4} (\delta_{xx} + \delta_{yy} - \delta_{zz}), \\ \sigma_{2y_{2\pm 1}}^0 &= -\sqrt{15/2} (\delta_{xz} \pm i\delta_{yz}), \\ \sigma_{2y_{2\pm 2}}^0 &= \sqrt{15/8} (\delta_{xx} - \delta_{yy} \pm 2i\delta_{xy}), \\ \sigma_{2y_{00}}^1 &= (\delta_{xx} + \delta_{yy} + \delta_{zz}). \end{aligned} \quad (21)$$

At a peak in the density field the peak slope is approximated by a parabolic function

$$\delta(\mathbf{x}) = \mathbf{x}_p - \frac{1}{2} \lambda_i (\mathbf{x} - \mathbf{x}_p)_i^2, \quad (22)$$

with the eigenvalues λ_i of the mass tensor $m_{ij} = -\delta_{ij}$ at the peak. If the boundary of the peak is given by the isodensity contour with $\delta = 0$, the inertia tensor can be written as

$$\mathbf{I} = \frac{\eta_0}{5} \Gamma \text{diag} (A_y^2 + A_z^2, A_x^2 + A_z^2, A_x^2 + A_y^2). \quad (23)$$

Here $A_i = \sqrt{2\delta/\lambda_i}$ are the ellipsoids semi-axes, Γ its volume and

η_0 its density, such that $M = \eta_0 \Gamma$ is the mass of the peak. In our approximation the density field is assumed to be homogeneous to first order and thus $\eta_0 = \Omega_m \rho_{\text{crit}} a^3$. We thus sample values for X^\pm from the joint covariance matrix of δ_{ij} and ψ_{ij} .

3.3 Decomposition of the shear tensor

As already mentioned, angular momentum will only be sourced by the anti-symmetric part of the matrix product X ; the Hodge dual to the angular momentum is the tensor

$$L_{ij} = a^2 \dot{D}_+ [I, \Psi]_{ij}. \quad (24)$$

Now, since the angular momentum can also be expressed as

$$L_i = I_{ij} \omega_j, \quad (25)$$

with angular velocity ω_j , we can conclude that

$$L_{ij} = I_{il} \omega_{lj}, \quad (26)$$

and thus, in matrix-vector notation

$$\omega = I^{-1} X^-. \quad (27)$$

For the shear we proceed in complete analogy, but using the anti-commutator instead of the commutator. In particular we thus decompose the tidal gravitational fields as follows:

$$\Psi = I^{-1} I \Psi = I^{-1} X^+ + I^{-1} X^- \equiv \tilde{\sigma} + \tilde{\omega}. \quad (28)$$

In a previous paper R16, we arrived at the following expressions for the shear and the rotation

$$\sigma = \Psi - \mathbb{I}_3 \Delta \psi, \quad \omega = \mathbf{0}, \quad (29)$$

where \mathbb{I}_3 is the identity matrix. Eqs. (28) and (29) agree identically if we subtract the trace of $\tilde{\sigma}$ from $\tilde{\sigma}$ and assume the protohalo to be spherical prior to the collapse, since in this case $X^- = \mathbf{0}$ and $X^+ = \Psi$. We thus write the shear and rotation which enter into the collapse equation as

$$\sigma = \frac{1}{2} (\Psi + I^{-1} \Psi I) - \frac{\text{tr} \Psi}{3} \mathbb{I}_3, \quad \omega = \frac{1}{2} (\Psi - I^{-1} \Psi I). \quad (30)$$

3.4 Calculation of the invariant $\sigma^2 - \omega^2$

The invariant quantities σ^2 and ω^2 just differ by the sign of the cross terms and by the terms which arise due to the term including the trace of Ψ . It is easy to see that the latter terms vanish identically, thus the only difference between σ^2 and ω^2 is the sign of the two cross term, which are themselves identical due to the cyclicity of the trace. In components:

$$\begin{aligned} 2\Psi_{ij}(I^{-1}\Psi I)_{ij} &= 2\Psi_{ij}I_{il}^{-1}\Psi_{la}I_{aj}, \\ &= 2\Psi_{ij}\tilde{\lambda}_l^{-1}\delta_{il}\Psi_{la}\lambda_{(a)}\delta_{aj}, \\ &= 2\frac{\tilde{\lambda}_j}{\lambda_i}\Psi_{ij}\Psi_{ij}, \end{aligned} \quad (31)$$

where we used Eq. (23) for the inertia tensor and that its eigenvalues are $\tilde{\lambda}_i$. For all physical situations we need to evaluate the inertia tensor at the maximum of a density field, as the definition of I would not be sensible otherwise. For the density field to have a maximum we must have $\lambda_i > 0$ and thus $\tilde{\lambda}_i > 0$ as well. We therefore arrive at the important conclusion that

$$2\Psi_{ij}(I^{-1}\Psi I)_{ij} \geq 0 \quad (32)$$

and thus $\sigma^2 \geq \omega^2$ provided the inertia tensor is positive semi-definite. Using the decomposition from Eq. (28) the value of the

term $\sigma^2 - \omega^2$ can directly be calculated using the random process outlined in the previous sections.

The outlined proof can be generalized to higher order invariants in a coordinate free way. We use that the invariants correspond to the Frobenius-norm of the tidal tensor and the inertia tensor. The Frobenius norm is defined as

$$\|A\|^2 = \text{tr} A^2 \equiv A_{ij} A^{ji} \quad (33)$$

of a symmetric matrix A . An inner product can be defined in the following way:

$$\langle A, B \rangle = \text{tr} AB = A_{ij} B^{ji}, \quad (34)$$

which is also called Frobenius scalar product, then inducing the Frobenius norm defined above. With this we find

$$\begin{aligned} \sigma^2 &= \|\langle I, \Psi \rangle\|^2 = \|I\Psi\|^2 + 2\langle I\Psi, \Psi I \rangle + \|I\Psi\|^2 \\ \omega^2 &= \|\langle I, \Psi \rangle\|^2 = \|I\Psi\|^2 - 2\langle I\Psi, \Psi I \rangle + \|I\Psi\|^2 \end{aligned} \quad (35)$$

Clearly, the positive definiteness of the Frobenius-norm implies that $\sigma^2 > \omega^2$ is fulfilled if $\langle I\Psi, \Psi I \rangle > 0$. Due to the cyclic property of the trace this term can be shown to be $\langle I\Psi, \Psi I \rangle = \text{tr}(I\Psi^2 I) = \text{tr}(I^2 \Psi^2) = \langle I^2, \Psi^2 \rangle$, which in turn is positive for positive (semi-) definite matrices I and Ψ .

To show this, one can use the generalisation of the inequality of the arithmetic and geometric mean,

$$\frac{1}{n} \langle I^2, \Psi^2 \rangle = \frac{1}{n} \text{tr}(I^2 \Psi^2) \geq (\det(I) \det(\Psi))^{1/n} \geq 0 \quad (36)$$

which is only valid for positive (semi-)definite matrices, with n being the dimension of the matrices. The tidal shear is positive definite at a peak of the density field, because $\text{tr}(\Psi) = \Delta \Psi = \delta > 0$ due to the Poisson-equation, and the inertia can only sensibly be defined at a maximum of the density field, where the curvature of the density field assumes positive values, resulting in a positive definite inertia $\text{tr}(I) > 0$. The argumentation applies for the traceless shear as well, as a positive semi-definite matrix. Both determinants are positive for positive definite matrices, and constrain the scalar product $\langle I^2, \Psi^2 \rangle$ to be larger than zero.

Figure 1 shows the effect mentioned in Eq. (32) very clearly: If we restrict the random process to maxima in the density field all values with $\sigma^2 < \omega^2$ disappear and get shifted to larger ratios of σ^2/ω^2 . Thus, gravitational tidal fields will always introduce more shear than rotation by tidal torquing if only maxima of the underlying density field are considered. This is indeed a necessary condition, since otherwise the inertia tensor would not be defined in a proper way. As a consequence the collapse will always proceed faster in a scenario with tidal gravitational fields than in a uniform background as it is the case for the SPC.

We show the, not normalized, joint distribution of σ^2 and δ in Figure 2. Due to the correlations in the y_{lm}^n basis given in Eq. (11), the maximum constraint enforces higher values in δ and σ^2 . In particular, peaks can only be found if $\delta > 0$, which is indeed necessary to write down the inertia tensor as in Eq. (23) as the ellipsoid is a region with boundary $\delta = 0$. Also the density peaks are significantly higher than without the constraint. Comparing these findings to R16 shows that in general the effect of shear will be reduced due to tidal torquing induced rotation. However, the rotation can never overcome the shear effect. Hence the term $\sigma^2 - \omega^2$ will become smaller than the pure σ^2 term in R16 as one can see on the left in Figure 3. It should be noted that the comparison between the invariants obtained in this work with those obtained in the previous paper is indeed difficult, as additional correlations are introduced due to the curvature in the density field. Also the decomposition of the

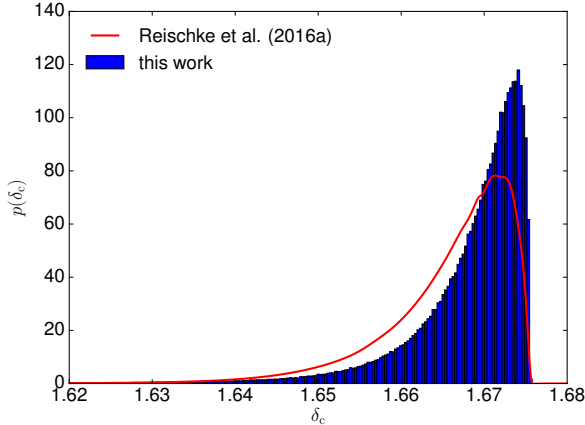


Figure 4. Distribution of the critical linear overdensity δ_c for a standard Λ CDM cosmology. The smoothing scale is again $R = 10\text{Mpc}h^{-1}$ and the density threshold is $\delta = 0$.

tidal tensor into a shearing and rotational part changes the magnitude of σ^2 . As mentioned earlier we would recover the result from the previous paper if \mathbf{I} would be proportional to the identity matrix, corresponding to spherical haloes. This effect will be discussed in more detail in the next section.

In the right panel of Figure 3 we show the distribution of $\sigma^2 - \omega^2$ with different thresholds for the overdensity δ at the peak. Clearly, higher overdensities at the peak imply higher shear values as the potential is more curved at higher peaks.

4 INFLUENCE ON δ_c , Δ_V AND SCALING PROPERTIES

In this section we investigate the influence of the tidal gravitational fields on the collapse dynamics by substituting the invariants σ^2 and ω^2 into the collapse equation. Additionally we will study the scaling with the mass of the collapsed structure. The cosmology is chosen to be a concordance Λ CDM model with $\Omega_m = 0.3$, $\Omega_\Lambda = 0.7$, $w = -1$, $h = 0.7$, $\sigma_8 = 0.8$ and $n_s = 0.96$.

In Figure 4 the resulting distribution of δ_c is shown. As expected we find similar results as in R16: The collapse always proceeds faster than in the case without tidal fields. As discussed in the previous section, this is due to the fact that the tidal field induced shear is always higher than the effect due to tidal torquing, provided we restrict our considerations to maxima in the density field. Thus the strong drop of the distribution at higher δ_c marks the value which one would get within a uniform background.

Due to the faster collapse, virialised objects form more easily, thus yielding more massive objects. This effect is similar to modified gravities theories or dark energy cosmologies with non-phantom dark energy. Since the distribution found for δ_c is similar to the one found in R16 and no significant differences were found for more complex dark energy models we refer to our previous works regarding the impact on the mass function and cluster counts.

As in R16 δ_c exhibits a mass dependence due to the low-pass filter with a scale R which is introduced to model the effective tidal fields acting on an object of size $R(M)$. The mass dependence changes slightly with respect to the mass dependence found in R16, since different spectral moments of the power spectrum enter into the random process. In particular they enter into the auto-

correlation in Eq. (11). We consider again the averaged values of the invariant $\sigma^2 - \omega^2$ or the linear critical density contrast δ_c .

On the left panel in Figure 5 we show the scaling of $\sigma^2 - \omega^2$ with respect to the mass (blue curve) obtained in this work and compare it to σ^2 from this and R16 in green and red, respectively. The general scaling with mass is the same for all curves, higher masses result into lower shear values as larger objects are only influenced by low frequency modes which become smaller for increasing scale. The invariant $\sigma^2 - \omega^2$ is only slightly smaller than σ^2 showing that the rotational term has only a minor impact on the collapse, which could already be expected from the general considerations about σ^2 and ω^2 before. We notice that the shear term only σ^2 is smaller than in the previous paper for masses below $10^{15} h^{-1} M_\odot$. The reason for this is that we considered before a random point in the density field, by smoothing it with a very broad kernel, as it is the case for high masses, it is likely to smooth over small fluctuations in the density field, thus reducing the tidal gravitational fields. In the case considered now we restrict ourselves to maxima in the density field thus the situation is constructed such that the curvature of the density field must be negative, thus yielding slightly more shear on large scales. On smaller scales, however, the situation is reversed. This argument is precisely due to the additional factor k^4 which enters in the random process for δ_{ij} (cf. Eqs. 9 and 21). Due to the same effect we find also a shallower slope of σ^2 in this case than before. Furthermore we notice that the combined effect of shear and rotation is smaller than the effect of shear only on all scales.

The right panel of Figure 5 shows the resulting scaling of δ_c . Here we additionally show the constant value (cyan curve) obtained without gravitational tidal fields. As for the invariants σ^2 and ω^2 the qualitative behaviour is identical. We find that the inclusion of tidal torquing slows down the collapse again on small scales compared to the results found in R16. However, on scales above $10^{14} M_\odot$ the curves approach each other, thus yielding a very similar (but slightly smaller) effect on the mass function and cluster counts than in our previous work.

As the underlying order of perturbation theory is the same as in our previous works the time evolution will be identical. For the evolution of δ_c with z we therefore refer to R16.

Another aspect that is interesting to investigate is the interplay between the dark energy equation of state w and the non-linear term $\sigma^2 - \omega^2$. As shown in R16, the shear term was rather insensitive to the particular dark energy model considered and giving for all the models considered approximately the same deviations as a function of mass and/or redshift. We can therefore perform a similar analysis taking into account the additional rotational term and compare our findings both with respect to the Λ CDM model and to the dark energy models analysed in R16 and Del Popolo et al. (2013b). When we do this, we once again notice that the combined effect of shear and rotation has a behaviour practically identical from a qualitative and a quantitative point of view to what shown in Figure 5 for the Λ CDM model. Deviations are small and at the percent level and decrease with increasing the mass. We find therefore that while in agreement with R16, we find an opposite trend with respect to Del Popolo et al. (2013b). This is because in our self-consistent approach the rotation term is always smaller than the shear term, while in Del Popolo et al. (2013b) the dominant term is by far the rotation one.

Finally we could also study how the term $\sigma^2 - \omega^2$ behaves in a more general setting, namely when dark energy clusters, as done in Pace et al. (2016). As shown there, the shear term had a very similar behaviour to smooth dark energy models, both quantitatively

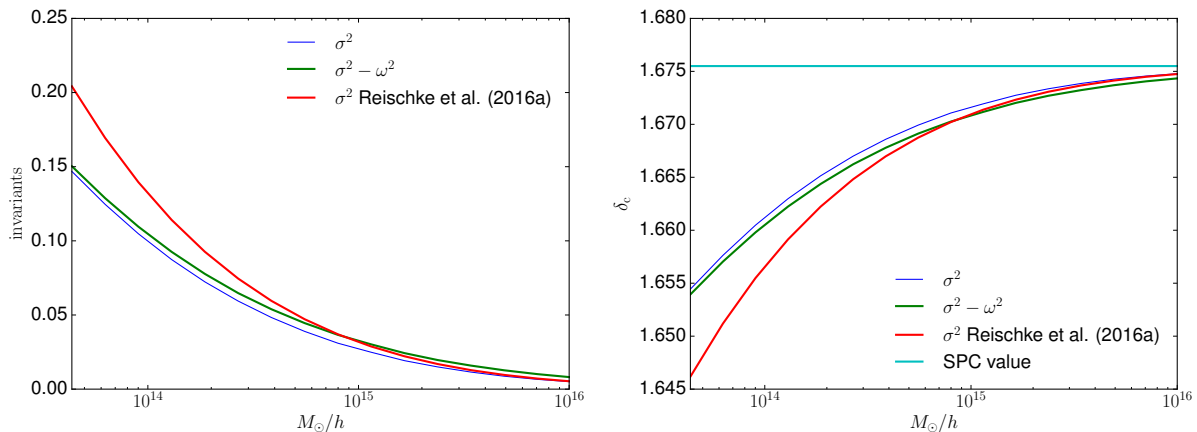


Figure 5. Scaling of the critical linear overdensity δ_c and the invariant $\sigma^2 - \omega^2$ as a function of mass. The influence of gravitational tidal fields is highest for low masses, thus δ_c is also influenced most at the low-mass tail.

and qualitatively; in addition it was completely insensitive to the fact that the shear term affected only the dark matter fluid or the dark energy fluid as well. Same situation happens here when we introduce the rotation term: we see that the qualitative and quantitative behaviour is practically identical to the smooth dark energy case and to the shear term only case. In addition, deviations when the rotation term is included are small, both when the term $\sigma^2 - \omega^2$ affects only dark matter or both dark matter and dark energy, as shown in Pace et al. (2014b).

This said, we therefore limit ourselves showing the results for the Λ CDM model only.

A very important and interesting quantity that can be evaluated within the framework of the spherical collapse model is the virial overdensity Δ_v , representing the overdensity of the collapsing object at the virialisation epoch (see also Meyer et al. 2012, for a discussion of this quantity in a general relativistic setting). The virial overdensity is also related to the size of spherically symmetric halos and its value can be inferred by embedding the virial theorem into the formalism.

When including the shear and the rotation terms into the equations of motion for dark matter perturbations, Δ_v becomes, in analogy to δ_c , mass-dependent. Repeating the analysis performed in R16, we can study its time- and mass-evolution also in this extended formalism. When we do this, it appears evident once more that Δ_v is practically independent of mass and it evolves as the system is perfectly symmetric. This is an interesting result but not unexpected. As we showed in R16, the virial overdensity is insensitive to mass since the quantities involved for its determination are evaluated still in the linear regime and perturbations with respect to the spherically symmetric case are of the order of per mill. Taking also into account that rotation has always a smaller contribution than the shear and their combined effect makes the rotating ellipsoid closer to the sphere in terms of the perturbation quantities, it is easy to understand why the feature found in R16 still holds.

5 CONCLUSION AND DISCUSSION

Extending the work of R16 we used the Zel'dovich approximation to model external tidal gravitational fields surrounding a spherical overdense region. By breaking the spherical symmetry prior to collapse and assuming the protohalo to be an ellipsoidal object with an

inertia tensor, sampled from the curvature of the density field, not proportional to the unit matrix, we can decompose the tidal tensor into a symmetric and antisymmetric part which can then be identified with a shear tensor and a rotational tensor. These tensors were used to construct the invariants σ^2 and ω^2 in the collapse equation. Physically the protohalo feels the tidal gravitational field and thus shear effects and also tidal torquing, as its inertia tensor eigensystem is not necessarily aligned with the one of the tidal tensor. This procedure is identical to the one presented in R16 if we restrict our considerations again to spherical objects which have an inertia tensor proportional to the unit matrix, which itself commutes with any other matrix. Our main findings are the following:

(i) The invariant quantity ω^2 of the rotational part of the tidal tensor is always smaller than the shear invariant σ^2 within the framework of tidal torquing if the considerations are restricted to maxima in the density field, which is necessary for all physically relevant cases. This statement is not of statistical nature, it is true for every sample individually.

(ii) The critical linear overdensity δ_c changes qualitatively in the same way as in R16. The mass dependence is slightly shallower and the overall effect is smaller at masses below $10^{15} M_\odot$ and completely negligible at masses above $10^{15} M_\odot/h$.

(iii) External tidal fields will always help objects to collapse into virialised structures even if a rotational term due to tidal torquing is considered. The influence on the mass function, cluster counts and cosmological parameters is roughly the same as in R16 and a collapse without tidal fields can in principles always be confused with dynamical dark energy increasing the abundance of heavy clusters in a purely spherically symmetric case where no tidal fields are taken into account.

(iv) Comparing this work with Del Popolo et al. (2013a) we find that the deviations of δ_c found there are mainly due to the rotational term, which can become rather large, thus the collapse is mostly slowed down. Our work finds an opposite result as the gravitational tidal fields always speed up the collapse and the rotational term is nearly negligible. This is, however, also a property of the model we used here. Our model is self-consistent in as long as we only consider external tidal effects on a spherically symmetric object where the deformation is negligible compared to the total extent of the collapsing object. In this work we assumed the halo to be non-spherical prior to collapse to allow it to spin up as long as the lever

arms are large enough. As soon as collapse starts, the collapse is again treated as being spherical. We therefore have a situation in which a spherically overdensity is rotating at an angular speed ω^2 gained by tidal torquing if it would have been an ellipsoidal object. These limitations make a direct comparison with Del Popolo et al. (2013a) difficult. See point (vi) for an explanation based on the way the invariant $\sigma^2 - \omega^2$ is evaluated.

(v) When comparing our results for clustering dark energy models with Pace et al. (2014b), once again we see that in our case the resulting effect is shear-dominated, while in Pace et al. (2014b) is rotation-driven. Therefore the comparison can only be done at a qualitative level. Effects are stronger at lower masses and redshifts where structures are more evolved. Reasons for the different behaviour are as explained in point (vi).

(vi) In our self-consistent model, the shear and rotation term have little effect and their effect grows with time and mass as structures evolve. In the formalism outlined, the invariant $\sigma^2 - \omega^2$ is evaluated at early times when structures are in the linear regime. This explains why, for example, the virial overdensity Δ_V is barely affected. In previous works on the subject (Del Popolo et al. 2013a,b; Pace et al. 2014b) instead, the term $\sigma^2 - \omega^2$ assumes objects to be still spherical in average and that the rotation term matches the present-day rotational velocity of clusters as a function of their mass. This late time evaluation makes the rotation term ω^2 the dominant one and this explains the different trends in the two series of papers.

(vii) In R16 we showed that the introduction of the shear term led to a $1-\sigma$ bias in the determination of the cosmological parameters, in particular Ω_m , σ_8 and w . Interestingly this bias was also in a direction which alleviates the tension between cluster and CMB data possible. Here we showed that, as expected, rotation slows down structure formation and therefore the bias would be alleviated slightly, increasing once again the tension between the two data sets.

6 ACKNOWLEDGEMENTS

RR acknowledges funding by the graduate college "Astrophysics of cosmological probes of gravity" by Landesgraduiertenakademie Baden-Württemberg. FP is supported by an STFC postdoctoral fellowship and thanks Inga Cebotaru for reading the manuscript and provide useful comments.

References

Abramo L. R., Batista R. C., Liberato L., Rosenfeld R., 2007, *Journal of Cosmology and Astro-Particle Physics*, 11, 12
 Abramo L. R., Batista R. C., Rosenfeld R., 2009, *Journal of Cosmology and Astro-Particle Physics*, 7, 40
 Angrick C., Bartelmann M., 2009, *Astronomy & Astrophysics*, 494, 461
 Avila-Reese V., Firmani C., Hernández X., 1998, *ApJ*, 505, 37
 Bernardeau F., 1994, *ApJ*, 433, 1
 Bertschinger E., 1985, *ApJS*, 58, 39
 Catelan P., Theuns T., 1996, *MNRAS*, 282, 436
 Cole S., et al., 2005, *MNRAS*, 362, 505
 Copeland E. J., Sami M., Tsujikawa S., 2006, *International Journal of Modern Physics D*, 15, 1753
 Crittenden R. G., Natarajan P., Pen U.-L., Theuns T., 2001, *ApJ*, 559, 552
 Del Popolo A., Pace F., Lima J. A. S., 2013a, *International Journal of Modern Physics D*, 22, 50038
 Del Popolo A., Pace F., Lima J. A. S., 2013b, *MNRAS*, 430, 628
 Diego J. M., Majumdar S., 2004, *MNRAS*, 352, 993

Fang W., Haiman Z., 2007, *Phys. Rev. D*, 75, 043010
 Fillmore J. A., Goldreich P., 1984, *ApJ*, 281, 1
 Gunn J. E., Gott III J. R., 1972, *ApJ*, 176, 1
 Heavens A. F., Sheth R. K., 1999, *Monthly Notices of the Royal Astronomical Society*, 310, 1062
 Komatsu E., Smith K. M., Dunkley J., et al. 2011, *ApJS*, 192, 18
 Lin C.-A., Kilbinger M., 2014, *Proceedings of the International Astronomical Union*, 10, 107
 Majumdar S., 2004, *Pramana*, 63, 871
 Maturi M., Angrick C., Pace F., Bartelmann M., 2010, *A&A*, 519, A23
 Maturi M., Fedeli C., Moscardini L., 2011, *Monthly Notices of the Royal Astronomical Society*, 416, 2527
 Meyer S., Pace F., Bartelmann M., 2012, *Phys. Rev. D*, 86, 103002
 Mota D. F., van de Bruck C., 2004, *A&A*, 421, 71
 Ohta Y., Kayo I., Taruya A., 2003, *ApJ*, 589, 1
 Ohta Y., Kayo I., Taruya A., 2004, *ApJ*, 608, 647
 Pace F., Waizmann J.-C., Bartelmann M., 2010, *MNRAS*, 406, 1865
 Pace F., Moscardini L., Crittenden R., Bartelmann M., Pettorino V., 2014a, *MNRAS*, 437, 547
 Pace F., Batista R. C., Del Popolo A., 2014b, *MNRAS*, 445, 648
 Pace F., Reischke R., Meyer S., Schäfer B. M., 2016, preprint, ([arXiv:1612.03018](https://arxiv.org/abs/1612.03018))
 Padmanabhan T., 1996, *Cosmology and Astrophysics through Problems* Perlmuter S., Aldering G., Goldhaber G., et al. 1999, *ApJ*, 517, 565
 Planck Collaboration et al., 2016, *A&A*, 594, A13
 Regős E., Szalay A. S., 1995, *Monthly Notices of the Royal Astronomical Society*, 272, 447
 Reischke R., Pace F., Meyer S., Schäfer B. M., 2016a, *MNRAS*,
 Reischke R., Maturi M., Bartelmann M., 2016b, *Monthly Notices of the Royal Astronomical Society*, 456, 641
 Riess A. G., Filippenko A. V., Challis P., et al. 1998, *AJ*, 116, 1009
 Ryden B. S., Gunn J. E., 1987, *ApJ*, 318, 15
 Schäfer B. M., 2009, *International Journal of Modern Physics D*, 18, 173
 Schäfer B. M., Koyama K., 2008, *Monthly Notices of the Royal Astronomical Society*, 385, 411
 Schäfer B. M., Merkel P. M., 2012, *Monthly Notices of the Royal Astronomical Society*, 421, 2751
 Sunyaev R. A., Zeldovich I. B., 1980, *ARA&A*, 18, 537
 White S. D. M., 1984, *ApJ*, 286, 38
 Zel'Dovich Y. B., 1970, *A&A*, 5, 84